ON THE SCALE-UP CRITERIA FOR BUBBLE COLUMNS

Giorgio Besagni[a], Lorenzo Gallazzini[b], Fabio Inzoli[c]

[a]*Politecnico di Milano, Department of Energy*

Via Lambruschini 4a, 20156 Milan, Italy

giorgio.besagni@polimi.it, lorenzo.gallazzini@mail.polimi.it and fabio.inzoli@polimi.it

ABSTRACT

It is generally admitted that experimental data obtained in "*laboratory-scale*" bubble columns are representative of "*industrial-scale*" reactors if the well-known three "*Wilkinson et al. scale-up criteria*" are satisfied: (a) the diameter of the bubble column is larger than 0.15 m, (b) the sparger openings are larger than 1-2 mm and (c) the aspect ratio is larger than 5. In this paper, we contribute to the existing discussion and we have experimentally studied the combined effect of the aspect ratio (within the range of 1-15) and the sparger design (considering both "*coarse*" and "*fine*" spargers) on the gas holdup in a large-diameter and large-scale gas-liquid bubble column. The bubble column has been operated both in the batch mode and in the counter-current mode. Filtered air has been used as the gaseous phase in all the experiments, while the liquid phase has included deionized water and different aqueous solutions of organic (i.e., ethanol) and inorganic (i.e., sodium chloride, NaCl) active agents. It is found that the "*Wilkinson et al. scale-up criteria*" are valid for the air-water case in the batch mode for "*very-coarse*" spargers. Conversely, they are no more valid when considering different liquid velocity, and/or aqueous solutions of active agents, and other sparger openings.

1. INTRODUCTION

Two-phase bubble columns are multiphase reactors where a gas phase is dispersed into a liquid phase in the form of disperse bubbles or of "*coalescence-induced*" bubbles. The two phases are separated by an interface, where interfacial transport phenomena may occur. The simplest bubble column configuration consists in a vertical cylinder, in which the gas enters at the bottom—through a gas sparger—and the liquid phase is supplied in batch mode or it may be led in either co-currently or counter-currently to the upward gas stream. Despite the simple bubble column design, complex fluid dynamics interactions and coupling between the phases, which manifest in the prevailing flow regimes [1], exist. Therefore, their correct design and operation rely on the proper prediction of the fluid dynamic properties: a typical approach is apply scale-up methods to estimate the fluid dynamics of "*industrial-reactor-scale*" reactors from "*laboratory-reactor-scale*" experimental facilities [2]. Subsequently, models for the interfacial mass transfer [3] and, eventually, to take into account the multi-phase reactions, are applied. The scale-up approaches from the "*laboratory-reactor-scale*" towards the "*industrial-reactor-scale*" rely on similarity criteria that would result in similar mixing and fluid dynamics and, hence, transport and performance in the two different scales. Many approaches were proposed and, in this respect, a pioneering study was proposed by Wilkinson et al. [4], after performing experiments in two different column diameters (d_c = 0.15 and d_c =

0.23 m), at different operating pressures and using different liquid phases (n-heptane, monoethylene glycol, and water). Based on their own results as well as on literature data, they concluded that the gas holdup is independent of the column dimensions and the gas sparger design if the following criteria (in the following, the "*Wilkison et al. scale-up criteria*") are satisfied:

1. **criterion 1.** The diameter of the bubble column, d_c, is larger than 0.15 m;
2. **criterion 2.** The aspect ratio, *AR* (the ratio between the height, H_0, and the diameter of the column, d_c), is larger than 5; despite some authors defined the aspect ratio in terms of the column height, the correct definition of *AR* strictly relies on the initial liquid level, as discussed by Sasaki et al. [5, 6] and demonstrated in this study.
3. **criterion 3**. The gas sparger openings diameter, d_o, is larger than 1-2 mm ("*coarse*" gas spargers).

The discussion concerning the large-diameter effects (*Wilkinson et al. scale-up criterion number 1*) was proposed in our previous papers (i.e., [7-9]) and is further proposed in Section 2. This paper contributes to the existing discussion on the scale-up criteria: it mainly focuses on the influence of the aspect ratio (*Wilkinson et al. scale-up criterion number 2*) and it also addresses the influence of the gas sparger design (*Wilkinson et al. scale-up criterion number 3*). In particular, in this paper we try to answer to a question: is a bubble column always subject to the "*Wilkinson scale-up criterion number 2*" or not? In this respect, this paper proposes an original point of view on the scale-up criteria, based on previously published experimental data as well as new data.

2. THE EXPERIMENTAL SETUP

The experimental facility (Figure 1) is a non-pressurized vertical pipe made of Plexiglas® with d_c = 0.24 m and H_c = 5.3 m. The column diameter classifies this facility as a large-diameter bubble column. The classification of large-diameter bubble column, is related to the fluid dynamic properties of the bubble columns itself and, in particular, it is related to the absence of the slug flow regime because of the Rayleigh–Taylor instabilities (see ref. [10]). The quantification of the Rayleigh–Taylor instabilities at the "*reactor-scale*" is quantified through the dimensionless diameter D^*_H, which is related to the Eötvös number of the slug bubbles as follows (See ref. [7, 8]):

$$D_H^* = \frac{D_H}{\sqrt{\sigma / g\left(\rho_L - \rho_G\right)}} \xrightarrow{\text{Circular bubble column}} \frac{d_c}{\sqrt{\sigma / g\left(\rho_L - \rho_G\right)}} = \\ = \frac{1}{\sqrt{\sigma / d_c^2 g\left(\rho_L - \rho_G\right)}} = \frac{1}{\sqrt{1/Eo_c}} = \sqrt{Eo_c} = \sqrt{Eo_{slug-bubble}} \quad (1)$$

In Eq. (1), D_H is the hydraulic diameter, d_c is the bubble column (inner) diameter, σ is the surface tension, g is the acceleration due to gravity, ρ_L - ρ_G is the density difference between the two phases, and Eo_c = $Eo_{slug\text{-}bubble}$ is the Eötvös number computed using the bubble column diameter, which is also the characteristic length of the slug bubbles. Bubble columns with D^*_H greater than the critical value $D^*_{H,cr}$ = 52 (accordingly with [11])—corresponding to $Eo_{slug\text{-}bubble}$ = 7.21 (i.e., $d_c \gtrsim$ 0.13-0.15 m; ambient temperature and pressure)—are considered to be large-diameter bubble columns. When the $d_c > D^*_{H,cr}$, the cap bubbles can no more be

sustained, and "*coalescence-induced*" bubbles (or cluster of bubbles) appear instead of the slug flow regime. The present bubble column has a dimensionless diameter D^*_H = 88.13 [7]. When the column diameter is larger than the critical value, the stabilizing effect of the channel wall on the interface of the Taylor bubbles decreases, and slug flow cannot be sustained anymore because of the Rayleigh-Taylor instabilities. The fluid dynamic properties in large-diameter columns differ from the flow in small-diameter columns and the flow regime maps and flow regime transition criteria used to predict the behavior of two-phase flow in small-diameter columns may not be scaled up to understand and predict the flow in large ones [12], in agreement with the scale-up criteria of Wilkinson et al. [4] and the flow map of Shah et al. [13]. The large diameter effects were described in our previous paper, to whom the reader may refer (see, for example, refs. [7, 9, 14]).

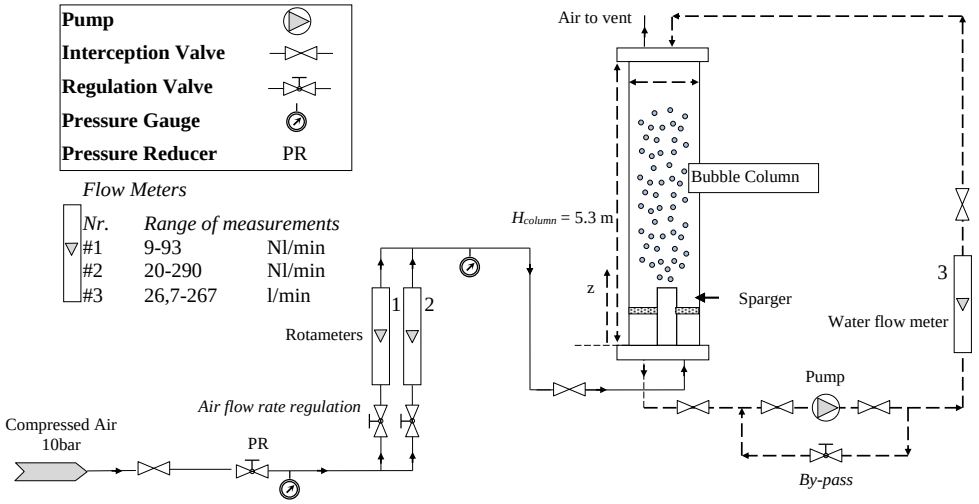

Figure 1. The experimental setup.

In the experimental facility, a pressure reducer controls the pressure upstream from the rotameters (1) and (2), used to measure the gas flow rate (accuracy ± 2% f.s.v., E5-2600/h, manufactured by ASA, Italy). A pump, controlled by a bypass valve, provides water recirculation, and a rotameter (3) measures the liquid flowrate (accuracy ±1.5% f.s.v., G6-3100/39, manufactured by ASA, Italy). Filtered air from laboratory lines has been used as the gaseous phase in all the experiments; the air-cleaning line consists in filters (mechanical and activated carbon) and condensation drying unit, in order to clean the gas phase properly and, thus, to avoid the presence of contaminants in form of (i) solid particles and (ii) organic substances. Conversely, the liquid phase has included deionized water and aqueous solutions of deionized water and (a) sodium chloride, (b) ethanol, to study the influence of the liquid properties on the bubble column fluid dynamics. The reader should refer to our previous studies for a more detailed discussion concerning the physical properties of the liquid phase, i.e., ref. [15]. In the present experimental investigation, the bubble column has been tested in the batch (U_L = 0 m/s) and in the counter-current (U_L = –0.0846 m/s) modes. The value of the liquid velocity has been selected taking into account our previous results and the literature. Indeed, low liquid velocities do not affect the gas holdup (see, for example, refs. [13, 16-23]) because, if U_L is low compared with the bubble rise velocities, the acceleration of the bubbles is negligible [24]. Conversely, at higher liquid velocities (as the one selected in the present study), the column operation influences the gas holdup: the co-current mode reduces the gas holdup, and the counter-current mode increases the gas holdup as bubbles are either accelerated or decelerated by liquid motion [14, 25-29]. The values of gas density (used to compute U_G) are based upon the operating conditions existing at the column midpoint

(computed by using the ideal gas law) [30]. The midpoint column pressure has been assumed equal to the column outlet pressure plus one-half the total experimental hydrostatic pressure head. Within this study, gas superficial velocities in the range between 0.004 (± 0.0005) and 0.23 (± 0.01) m/s have been considered, where the uncertainties were evaluated at 95% confidence. To test the influence of the gas sparger design, two spargers have been tested:

- **Spider sparger (‘*coarse*’ sparger)**. The spider sparger, shown in Figure 2a, has six arms made of 0.12 m diameter stainless steel tubes soldered to the center cylinder of the sparger. The sparger has been installed with the six holes (d_o = 2 - 4 mm) located on the side of each arm facing upward, with an increasing diameter moving toward the column wall. This sparger is an example of an industrial sparger. The reader should refer to our other papers for other photos and description of the spider sparger design [7, 8, 31].

- **Perforated place sparger (‘*fine*’ sparger).** This sparger, shown in Figure 2b, has been designed to produce smaller bubbles (because of the small sparger opening and the mechanics of the bubble growing) and generate stable and mono-dispersed homogeneous flow regime. The sparger consists in a sparger zone and a plenum. The sparger zone consists of plates with 581 holes, with holes having 1.0 mm inner diameter, uniformly distributed about the column cross-section. The plenum, built in Plexiglas®, is 0.21 diameter and 0.21 m height.

The two gas spargers are both representative of the “*Wilkinson et al. scale-up criterion number 3*”, and have been selected to understand the range of validity of the “*Wilkinson et al. scale-up criterion number 2*”.

(a) Spider sparger **(b) Perforated plate sparger**

Figure 2. Gas spargers tested.

3. THE EXPERIMENTAL PROCEDURE: GAS HOLDUP MEASUREMENTS

The gas holdup (ε_G) is a dimensionless parameter defined as the volume of the gas phase divided by the total volume. Measurements of the bed expansion allowed the evaluation of ε_G: the procedure involves measuring the location (height) of the liquid free surface when air flows in the column. The gas holdup is then obtained using Eq. (2):

$$\varepsilon_G = \frac{V_G}{V_{L+G}} \xrightarrow{\text{Constant cross-section-area}} \frac{\left(H_D - H_0\right)}{H_D} \qquad (2)$$

Where V_G is the volume of the dispersed phase, V_{L+G} is the total volume, H_D is the height of the free-surface after aeration and H_0 is the height of the free-surface before aeration. H_0 is varied in order to study the influence of different AR (in the range $1 \leq AR \leq 15$). Height measurements are performed from gas sparger opening as reference location.

4. THE EXPERIMENTAL RESULTS

Herein, the experimental results are presented and discussed. It is worth noting that the discussion of the results is mainly focused on the role of the aspect ratio and the reader should refer to our previous papers (cited in the following sections) for a more detailed comparison with the previous literature as well as the discussion concerning the flow regime transitions.

4.1 Preliminary considerations on the influence of the aspect ratio

Generally, the bubble size distribution imposed by the gas sparger evolves in the axial direction of the bubble column and, in the systems where the bubble sizes are not at their maximum equilibrium size (and where coalescence may occur), the liquid height will influence the extent of the coalescence. Consequently, the gas holdup would decrease with the liquid height. In fact the higher the column, the longer the time the bubbles have to coalesce and, thus, the lower the mean residence time of the gas phase. Furthermore, in shorter bubble columns, the liquid circulation patterns (that tends to decrease the gas holdup) are not fully developed and the end-effects are more evident.

4.2 Air-water in batch mode: influence of the gas sparger design

Figure 3 displays the gas holdup curves in the batch mode for the different *ARs* (in the range $1 \leq AR \leq 15$) for the spider sparger and the perforate plate sparger. For further details the reader may refer to ref. [32].

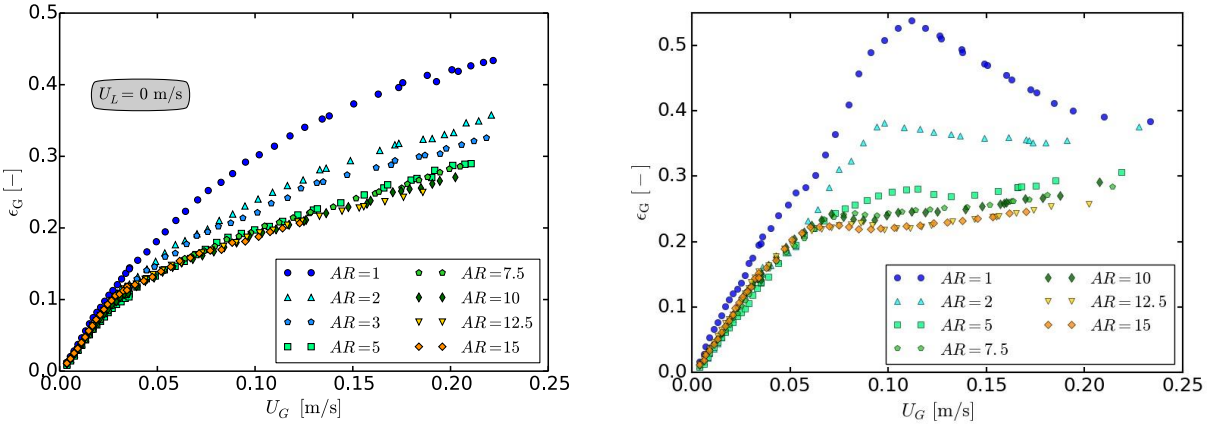

(a) Batch mode – Data taken from ref. [32]

(b) Batch mode – New experimental data

Figure 3. Gas holdup curves: influence of the gas sparger design.

Spider sparger (Figure 3a). The spider sparger leads to monotonic gas holdup curves concave in shape, which is well described in refs. [7-9] by considering hindrance effects in "*coarse sparger*" bubble columns. This shape of the gas holdup curve is mainly related to the large sparger openings, thus producing the "*pseudo-homogeneous*" flow regime (as also

described and quantified by the image analysis in our previous papers). At low U_G, in the "*pseudo-homogeneous*" flow regime, the relationship between ε_G and U_G is linear, followed by a change in slope due to the flow regime transition. After the flow regime transition, the appearance of "*coalescence-induced*" bubbles increases the average rise velocity of the dispersed phase and reduces the mean gas residence time in the bubble column, thus reducing the gas holdup versus gas velocity slope. The gas holdup decreases continuously while increasing *AR* up to the critical aspect ratio, AR_{Cr} = 5. Above AR_{Cr}, there is no remarkable difference in the gas holdup curves. The value of the critical aspect ratio, AR_{Cr} = 5, is in agreement with the scale-up criteria of Wilkinson et al. [4].

Perforated plate sparger (Figure 3b). The perforated plate sparger produces the "*mono-dispersed homogeneous*" flow regime and leads to a *S-shaped* gas holdup curve. This shape of the gas holdup curve is related to the hindrance effects on the mono-dispersed bubble size distribution [33, 34]: the gas holdup curve passes through the maximum increasing U_G, then decreases, and then gas holdup once again increases with U_G. We may identify four different regions: (a) "*mono-dispersed homogeneous*" flow regime; (b) a "*pseudo-homogeneous"* flow regime; (c) a transition flow regime (around the maximum of the gas holdup curve); (d) the heterogeneous flow regime. The detailed description of these flow regimes will be discussed in future papers. To the authors' opinion, the *S-shaped* operation curve can be better understood if considering the Ledinegg instability, which is representative of the instabilities due to the pressure drop-flow rate (i.e., ε_G and U_G). The gas holdup decreases continuously while increasing *AR* up to the critical aspect ratio, AR_{Cr} = 10. Above AR_{Cr}, there is no remarkable difference in the gas holdup curves. The value of the critical aspect ratio, AR_{Cr} = 10, is higher compared with with the scale-up criteria of Wilkinson et al. [4].

4.3 Air-water: counter-current mode

Figure 4 displays the gas holdup curves in the counter-current mode (U_L = -0.0846 m/s) for the different *ARs* (in the range $5 \leq AR \leq 15$) for the spider sparger. For further details the reader may refer to ref. [32].

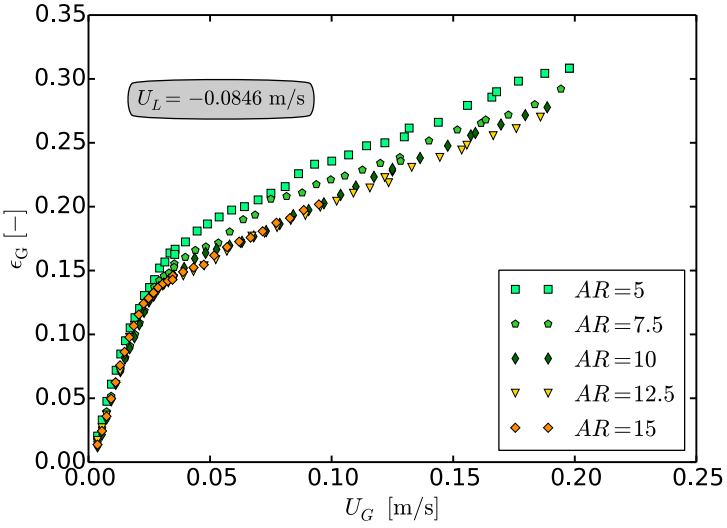

Figure 4. Gas holdup curves: influence of the counter-current mode - Data taken from ref. [32].

Compared with the batch mode, upon increasing the liquid flow rate, a faster increase in the gas holdup has been observed at low U_G. This change is explained by the effect of the liquid

flow, which slows down the rise of the bubbles, leading to higher gas holdup. The gas holdup decreases continuously while increasing *AR* up to the critical aspect ratio, AR_{Cr} = 10. Above AR_{Cr}, there is no remarkable difference in the gas holdup curves. The value of the critical aspect ratio, AR_{Cr} = 10, is higher compared with the scale-up criteria of Wilkinson et al. [4]. The increase in AR_{Cr} in counter-current mode can be explained by the increase in the coalescence phenomena. In the counter-current mode, the lower bubble rising velocity causes higher gas holdup and, thus, the more compact arrangement of bubbles leads to higher coalescence rate [7, 9].

4.4 Air-water-NaCl

Figure 5 displays the gas holdup curves in the batch mode for the different *ARs* (in the range 5 ≤ AR ≤ 12.5) for the NaCl concentrations, for the spider sparger. For further details the reader may refer to ref. [32]. Please note that the data have been presented in terms of the non-dimensional concentration (*n**), defined as the ratio between the molar NaCl concentration and the critical concentration value equal to n_t = 0.145 mol/l [35] (see refs. [31] for a more detailed discussion on the concept of the non-dimensional concentration). In our previous paper we have shown how the gas holdup grows continuously and non-linearly while increasing the electrolyte concentration, up to a certain value of the NaCl concentration. In this respect, it is worth noting that the non-linearity of the electrolytes effect upon the gas holdup suggest that the fluid dynamics in bubble columns having a binary liquid phase can not be entirely explained and modeled by using the bulk physical properties of the liquid phase. When considering these experimental data, it is worth noting that the data obtained in ref [31, 36] are slightly below the ones in ref. [32]; indeed, despite the great care in the experimentations, some factors may affect the experimental results conducted in different time periods, especially in a large-scale experimental facility: the reader please refer to the discussion proposed in ref. [32] for a comprehensive discussion on this issue. Taking into account this uncertainty, we may reasonably state that the gas holdup decreases continuously while increasing *AR* up to a critical aspect ratio, which is equal or greater than 10 ($AR_{Cr} \geq 10$), which is higher compared with the scale-up criteria of Wilkinson et al. [4]. These results have clearly demonstrated how coalescence phenomena strongly affect the influence of *AR* on the bubble column fluid dynamics (it is well-known that electrolytes suppress coalescence, as also stated and reviewed in our previous papers, i.e., refs. [31]).

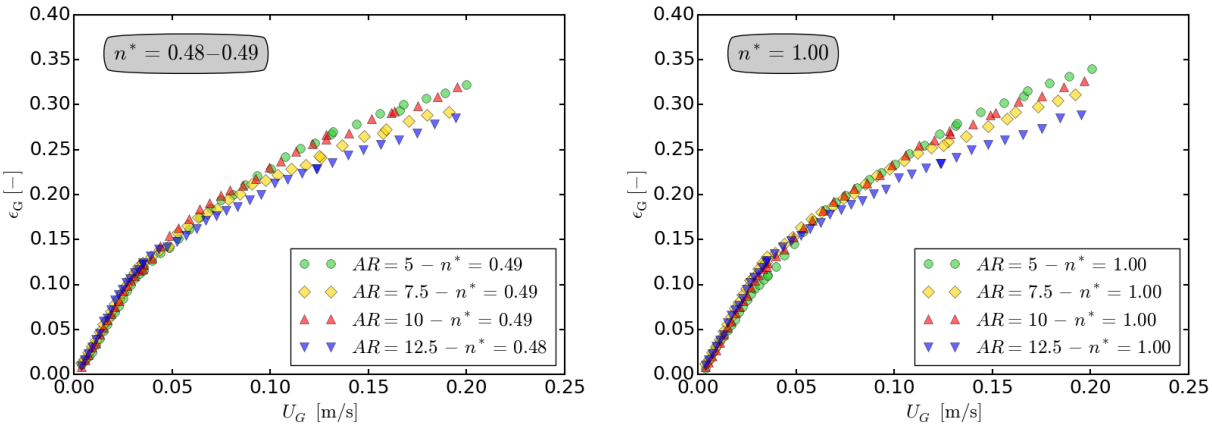

(a) Influence of *AR* on ε_G (*n = 0.48 – 0.49) – Data taken from ref. [32]**

(b) Influence of *AR* on ε_G (*n = 1.00) – Data taken from ref. [32]**

Figure 5. Gas holdup curves: influence of NaCl concentration.

4.5 Air-water-EtOH

Figure 6 displays the gas holdup curves in the batch mode for the different *ARs* (in the range 5 ≤ *AR* ≤ 12.5) for the EtOH concentrations, for the spider sparger. For further details the reader may refer to refs. [15, 37].

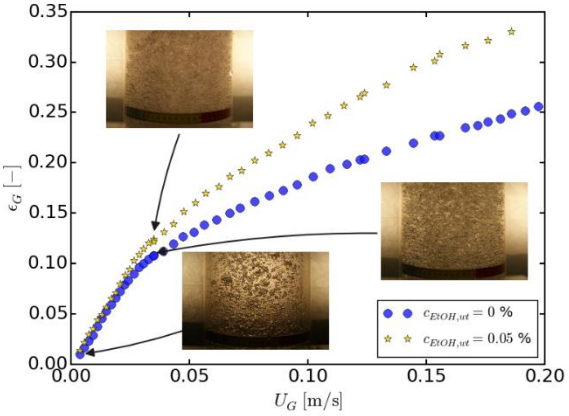

(a) *AR* = 12.5 – Data taken from ref. [37]

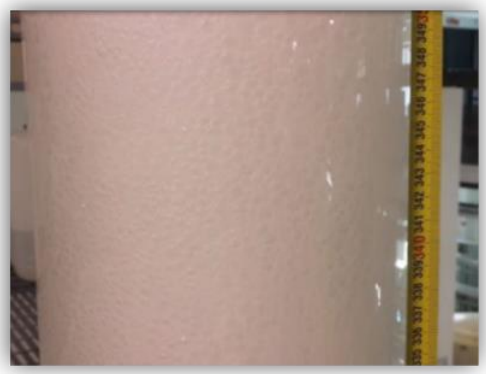

(b) *AR* = 10 - $c_{EtOH,wt}$ = 0.3 % Foaming phenomena

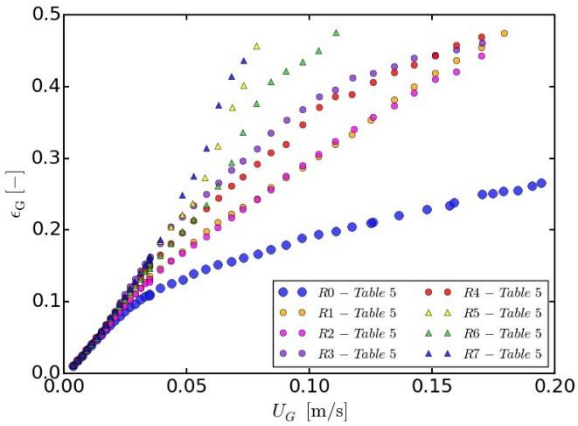

(c) *AR* = 10 – $c_{EtOH,wt}$ = 0.3 % – Data taken from ref. [15]; Foaming cases - Code reference in Table 1

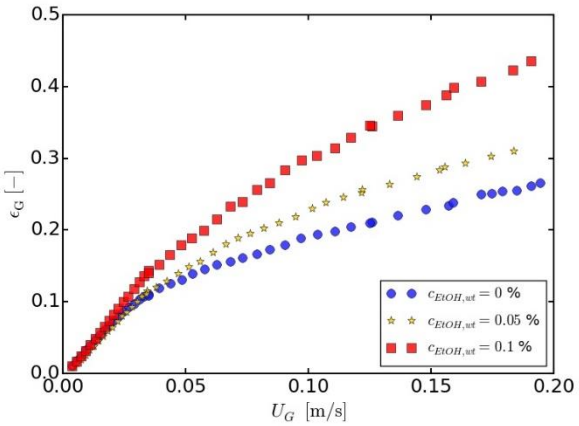

(d) *AR* = 10 – $c_{EtOH,wt}$ = 0 – 0.1 % – Data taken from ref. [15]; Non foaming cases

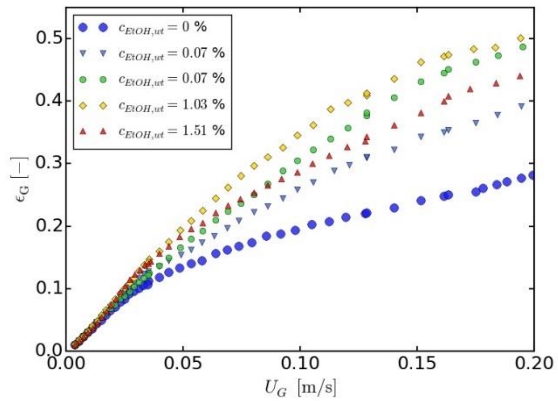

(e) *AR* = 7.5 – $c_{EtOH,wt}$ = 0 – 1.51 % – Data taken from ref. [15]; Non foaming cases

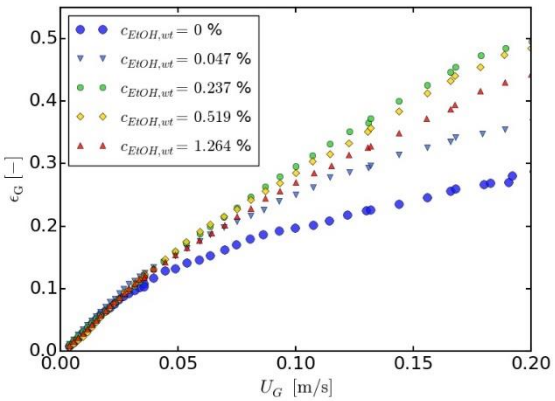

(f) *AR* = 5 – $c_{EtOH,wt}$ = 0 – 1.264 % – Data taken from ref. [15]; Non foaming cases

Figure 6. Gas holdup curves and foaming phenomena: influence of EtOH concentration.

First, the gas holdup measurements obtained in ref. [37] are discussed (Figure 6a, 0.05 $\%_{wt}$ ethanol concentration at AR = 12.5); second, the gas holdup measurements presented in ref. [15] are discussed, to study a broader range of ethanol concentrations and *ARs*, to provide insights in foaming phenomena (Figure 6b, 6c, 6d, 6e and 6f). The former case (0.05 $\%_{wt}$, AR = 12.5), has been widely investigated in our previous studied also concerning bubble size distributions, where we discussed how, compared with air-water system, the gas holdup increases with the addition of ethanol. Starting from this case (0.05 $\%_{wt}$, AR = 12.5), if the ethanol concentration is further increased, foam phenomena were observed. The reader should refer to the discussion proposed by Besagni and Inzoli [15] for the description of the flow regimes in bubble column with a foaming liquid phase. For example, at AR = 10, foam phenomena were observed: at the top of the column the formation of a thick cap of foam was noted (Figure 6b) the cap prevented air escape, causing bubble accumulation and a significant gas holdup growth (more than 50%, in some cases). The increase of ε_G when decreasing AR is verified for the air-water systems and for the ethanol-water system at AR = 5 and 7.5 (where foaming phenomena were not observed, Figure 5a). At AR = 5 and 7.5, the gas holdup increases continuously and non-linearly with ethanol concentration, which agrees with the previous literature. At AR = 10, the gas holdup increases while increasing the ethanol concentration without foaming up to a certain concentration; at concentrations equal or higher than 0.3 $\%_{wt}$, foam has been observed. In order to provide insights in foaming phenomena, many experiments were conducted at controlled conditions, to ensure that all the boundary conditions that may affect the results were checked: the results are displayed in Figure 6c and the code references are displayed in Table 1. *R1* and *R2* gas holdup curves (Figure 6c) are very similar, suggesting that when foaming was not observed, the gas holdup curve is unique. *R3* gas holdup curve, obtained in the same testing session of *R1* shows a hysteretic behavior, that was never observed with air-water systems. *R4* gas holdup curve suggests that the gas holdup depends on time: the gas holdup values in this curve are higher than the ones of *R1* and *R2*. The *"foaming"* gas holdup curves (*R5*, *R6* and *R7*), show that, when foaming occurs, gas holdup undergoes a pseudo-linear growth reaching very high values at relatively low superficial gas velocity; in this cases, no repeatability is observed. It is interesting that, once fixed flow rate and *AR*, gas holdup seems to be time dependent (R4 gas holdup curve). It is worth noting that foaming occurs approximately after the first flow regime transition, which is in agreement with the predictions of Shah et al. [38], that estimated the appearing of foaming at approximately U_G = 0.03 – 0.04 m/s.

Table 1. Code reference for Figure 6.

Code	Description
R0	$c_{EtOH,wt}$ = 0 % - Air-water gas holdup curve
R1	$c_{EtOH,wt}$ = 0.3 % - Gas holdup curve measured waiting 30 seconds for every gas holdup measurement point, from low to high gas flow rate – run 1
R2	$c_{EtOH,wt}$ = 0.3 % - Gas holdup curve measured waiting 30 seconds for every gas holdup measurement point, from low to high gas flow rate – run 2
R3	$c_{EtOH,wt}$ = 0.3 % - Gas holdup curve measured waiting 120 seconds for every gas holdup measurement point, from high to low gas flow rate
R4	$c_{EtOH,wt}$ = 0.3 % - Gas holdup curve measured waiting 120 seconds for every gas holdup measurement point, after each flow rate increase
R5	$c_{EtOH,wt}$ = 0.3 % - Gas holdup curve when foaming phenomenon was observed – Run 1
R6	$c_{EtOH,wt}$ = 0.3 % - Gas holdup curve when foaming phenomenon was observed – Run 2
R7	$c_{EtOH,wt}$ = 0.3 % - Gas holdup curve when foaming phenomenon was observed – Run 3

5. CONCLUSIONS ON THE SCALE-UP CRITERIA

This paper contributes to the existing discussion on the scale-up criteria for bubble columns, based on previously published experimental data as well as new experimental data. This paper mainly focuses on the influence of the aspect ratio (*Wilkinson et al. scale-up criterion number 2*) and it also addresses the influence of the gas sparger design (*Wilkinson et al. scale-up criterion number 3*). In particular, in this paper we try to answer to a question: is a bubble column always subject to the "*Wilkinson et al. scale-up criterion number 2*" or not?

The main results are as follows:

1. the value of AR_{Cr} depends on the gas sparger design;
2. the value of AR_{Cr} depends on the operation modes;
3. the value of AR_{Cr} depends on the liquid phase properties;
4. foaming phenomena were observed for organic active compounds in the case of high aspect ratios only. Foaming phenomena were not observed for low aspect ratios.

Therefore, our answer to the above-mentioned question is as follow: based on the obtained experimental results, we may conclude that the "*Wilkinson scale-up criterion number 2*" (AR_{Cr} = 5) is ensured only for air-water systems, with very large sparger openings ("*very-coarse*" spargers).

6. FUTURE WORKS

It has not escaped our notice that, in a very recent study, Sasaki et al. [6] investigated a large-diameter bubble columns at low-intermediate *AR* (d_C in the range of 0.16 – 0.3 m - *AR* up to 6.5) and a very-large-diameter bubble column at low *AR* (d_C = 2 m - *AR* up to 2). They concluded that the gas holdup is independent of the column design in large-diameter and high *AR* bubble columns; in particular, they stated as follows: "*the effects of d_c and H_0 on ε_G are negligible when scaling up from small to large bubble columns, provided that α_G in the small columns are obtained for $d_C \geqslant 200$ mm and $H_0 \gtrsim 2200$ mm. The height-to-diameter ratio is useless in evaluation of the critical height, above which ε_G does not depend on H_0.*". Conversely, we support the use of *AR* as scale-up criteria. It is worth noting that Sasaki et al. [6] studied a very-large-diameter bubble column (having $d_c >> 0.15$ m; where, 0.15 m is the threshold value stated by the "*Wilkinson et al. scale-up criterion number 1"*) and our experimental setup has $d_c = 0.24$ m > 0.15 m. Future researchers are encouraged to perform similar experimental investigations in very-large-diameter and high *AR* bubble column in order to clarify where our proposal or the proposal of Sasaki et al. is to be further pursued in the future research.

REFERENCES

[1] S.K. Majumder, Hydrodynamics and Transport Processes of Inverse Bubbly Flow, Elsevier Inc., 2016.
[2] A. Shaikh, M. Al-Dahhan, Scale-up of Bubble Column Reactors: A Review of Current State-of-the-Art, Industrial & Engineering Chemistry Research, 52 (2013) 8091-8108.
[3] R. Rzehak, Modeling of mass-transfer in bubbly flows encompassing different mechanisms, Chemical Engineering Science, 151 (2016) 139-143.

[4] P.M. Wilkinson, A.P. Spek, L.L. van Dierendonck, Design Parameters Estimation for Scale-Up of High-Pressure Bubble Columns, A.I.Ch.E. Journal, 38 (1992) 544-554.
[5] S. Sasaki, K. Hayashi, A. Tomiyama, Effects of liquid height on gas holdup in air–water bubble column, Experimental Thermal and Fluid Science, 72 (2016) 67-74.
[6] S. Sasaki, K. Uchida, K. Hayashi, A. Tomiyama, Effects of column diameter and liquid height on gas holdup in air-water bubble columns, Experimental Thermal and Fluid Science, 82 (2017) 359-366.
[7] G. Besagni, F. Inzoli, Comprehensive experimental investigation of counter-current bubble column hydrodynamics: holdup, flow regime transition, bubble size distributions and local flow properties, Chemical Engineering Science, 146 (2016) 259–290.
[8] G. Besagni, F. Inzoli, G. De Guido, L.A. Pellegrini, The dual effect of viscosity on bubble column hydrodynamics, Chemical Engineering Science, 158 (2017) 509-538.
[9] G. Besagni, F. Inzoli, Influence of internals on counter-current bubble column hydrodynamics: Holdup, flow regime transition and local flow properties, Chemical Engineering Science, 145 (2016) 162-180.
[10] J. Kitscha, G. Kocamustafaogullari, Breakup criteria for fluid particles, International Journal of Multiphase Flow, 15 (1989) 573-588.
[11] C.S. Brooks, S.S. Paranjape, B. Ozar, T. Hibiki, M. Ishii, Two-group drift-flux model for closure of the modified two-fluid model, International Journal of Heat and Fluid Flow, 37 (2012) 196-208.
[12] M.E. Shawkat, C.Y. Ching, Liquid Turbulence Kinetic Energy Budget of Co-Current Bubbly Flow in a Large Diameter Vertical Pipe, Journal of Fluids Engineering, 133 (2011) 091303-091303.
[13] Y.T. Shah, B.G. Kelkar, S.P. Godbole, W.D. Deckwer, Design parameters estimations for bubble column reactors, AIChE Journal, 28 (1982) 353-379.
[14] G. Besagni, G.R. Guédon, F. Inzoli, Annular Gap Bubble Column: Experimental Investigation and Computational Fluid Dynamics Modeling, Journal of Fluids Engineering, 138 (2016) 011302.
[15] G. Besagni, F. Inzoli, The effect of liquid phase properties on bubble column fluid dynamics: Gas holdup, flow regime transition, bubble size distributions and shapes, interfacial areas and foaming phenomena, Chemical Engineering Science, In Press (2016).
[16] K. Akita, F. Yoshida, Gas Holdup and Volumetric Mass Transfer Coefficient in Bubble Columns. Effects of Liquid Properties, Industrial & Engineering Chemistry Process Design and Development, 12 (1973) 76-80.
[17] J. Voigt, K. Schügerl, Absorption of oxygen in countercurrent multistage bubble columns—I Aqueous solutions with low viscosity, Chemical Engineering Science, 34 (1979) 1221-1229.
[18] P. Rollbusch, M. Becker, M. Ludwig, A. Bieberle, M. Grünewald, U. Hampel, R. Franke, Experimental investigation of the influence of column scale, gas density and liquid properties on gas holdup in bubble columns, International Journal of Multiphase Flow, 75 (2015) 88-106.
[19] A. Sangnimnuan, G.N. Prasad, J.B. Agnew, Gas Hold-Up and Backmixing in a Bubble-Column Reactor Under Coal-Hydroliquefaction Conditions, Chemical Engineering Communications, 25 (1984) 193-212.
[20] T.J.W. de Bruijn, J.D. Chase, W.H. Dawson, Gas holdup in a two-phase vertical tubular reactor at high pressure, The Canadian Journal of Chemical Engineering, 66 (1988) 330-333.
[21] R. Lau, W. Peng, L.G. Velazquez-Vargas, G.Q. Yang, L.S. Fan, Gas-Liquid Mass Transfer in High-Pressure Bubble Columns, Industrial and Engineering Chemistry Research, 43 (2004) 1302-1311.

[22] G.Q. Yang, L.S. Fan, Axial liquid mixing in high-pressure bubble columns, AIChE Journal, 49 (2003) 1995-2008.
[23] A.T. Shawaqfeh, Gas holdup and liquid axial dispersion under slug flow conditions in gas–liquid bubble column, Chemical Engineering and Processing: Process Intensification, 42 (2003) 767-775.
[24] J.H. Hills, The operation of a bubble column at high throughputs: I. Gas holdup measurements, The Chemical Engineering Journal, 12 (1976) 89-99.
[25] M.S. Baawain, M.G. El-Din, D.W. Smith, Artificial neural networks modeling of ozone bubble columns: Mass transfer coefficient, gas hold-up, and bubble size, Ozone: Science and Engineering, 29 (2007) 343-352.
[26] A.K. Bin, B. Duczmal, P. Machniewski, Hydrodynamics and ozone mass transfer in a tall bubble column, Chemical Engineering Science, 56 (2001) 6233-6240.
[27] H. Jin, S. Yang, G. He, M. Wang, R.A. Williams, The effect of gas-liquid counter-current operation on gas hold-up in bubble columns using electrical resistance tomography, Journal of Chemical Technology & Biotechnology, 85 (2010) 1278-1283.
[28] T. Otake, S. Tone, K. Shinohara, Gas holdup in the bubble column with cocurrent and countercurrent gas-liquid flow, Journal of Chemical Engineering of Japan, (1981) 338-340.
[29] G. Besagni, G. Guédon, F. Inzoli, Experimental investigation of counter current air-water flow in a large diameter vertical pipe with inners, Journal of Physics: Conference Series, 547 (2014) 012024.
[30] I. Reilly, D. Scott, T. Debruijn, D. MacIntyre, The role of gas phase momentum in determining gas holdup and hydrodynamic flow regimes in bubble column operations, The Canadian Journal of Chemical Engineering, 72 (1994) 3-12.
[31] G. Besagni, F. Inzoli, The effect of electrolyte concentration on counter-current gas-liquid bubble column fluid dynamics: gas holdup, flow regime transition and bubble size distributions, Chemical Engineering Research and Design, 118 (2017) 170–193.
[32] G. Besagni, A.D. Pasquali, L. Gallazzini, E. Gottardi, L.P.M. Colombo, F. Inzoli, The effect of aspect ratio in counter-current gas-liquid bubble columns: experimental results and gas holdup correlations, International Journal of Multiphase Flow, In Press (2017).
[33] S. Sharaf, M. Zednikova, M.C. Ruzicka, B.J. Azzopardi, Global and local hydrodynamics of bubble columns – effect of gas distributor, Chemical Engineering Journal, 288 (2016) 489–504.
[34] M.C. Ruzicka, J. Zahradník, J. Drahoš, N.H. Thomas, Homogeneous–heterogeneous regime transition in bubble columns, Chemical Engineering Science, 56 (2001) 4609-4626.
[35] J. Zahradník, M. Fialová, V. Linek, The effect of surface-active additives on bubble coalescence in aqueous media, Chemical Engineering Science, 54 (1999) 4757-4766.
[36] B. Giorgio, I. Fabio, Influence of electrolyte concentration on holdup, flow regime transition and local flow properties in a large scale bubble column, Journal of Physics: Conference Series, 655 (2015) 012039.
[37] G. Besagni, F. Inzoli, G. De Guido, L.A. Pellegrini, Experimental investigation on the influence of ethanol on bubble column hydrodynamics, Chemical Engineering Research and Design, 112 (2016) 1-15.
[38] Y.T. Shah, S. Joseph, D.N. Smith, J.A. Ruether, On the behavior of the gas phase in a bubble column with ethanol-water mixtures, Industrial & Engineering Chemistry Process Design and Development, 24 (1985) 1140-1148.